The background of the slide features a complex, turbulent plasma simulation. It consists of a dense network of magnetic field lines and plasma filaments, rendered in shades of red, orange, yellow, and black against a white background. The filaments are highly convoluted and chaotic, representing the non-linear dynamics of the astrophysical system.

Intermittency in multi-phase astrophysical dynamos

Fred Gent, (Aalto University - Astroinformatics)
Mordecai-Mark Mac Low, Maarit Käpylä, Nishant Singh

May 17, 2021 – Pencil Code User Meeting, EPFL

Galactic dynamo - large and small scale

(Gent et al. 2013)

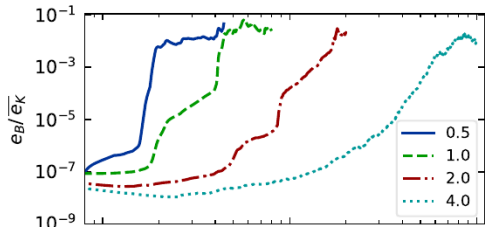
(Gressel et al. 2008, Gressel
& Elstner 2020)

(Korpi et al. 1999, Hanasz
et al. 2009, Wang &
Abel 2009, Rieder &
Teyssier 2016, Rieder &
Teyssier 2017a, Rieder &
Teyssier 2017b, Pakmor
et al. 2017, Steinwandel
et al. 2019) show no LSD or
LSD without SSD.

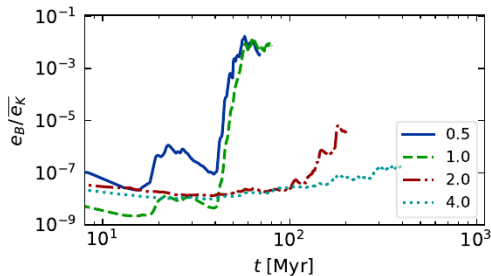
Small-scale dynamo (SSD) – Experimental setup

- ▶ 3D periodic ISM 1 ppcc 256(200) pc on each side
- ▶ SN rate comparable to solar neighbourhood $0.2 - 8 \dot{\sigma}_{\text{sn}}$
- ▶ Energy: radiative cooling and UV-heating, hyperdiffusion and shock diffusion
- ▶ Induction: hyperdiffusion and $\eta \in [0, 0.05] \text{ kpc km s}^{-1}$
- ▶ Momentum: hyperdiffusion and shock diffusion
 $\nu \in [0, 0.001]$
- ▶ Continuity: shock diffusion
- ▶ Resolution 0.5, 1, 2 and 4 pc

Magnetic energy growth rates



Magnetic energy density for resolutions $\delta x = 0.5\text{--}4$ pc,
scaled to time-averaged kinetic energy density \bar{e}_K



for resistivity (a) $\eta = 10^{-4}$ & (b)
 $10^{-3} \text{ kpc km s}^{-1}$.

Dependence on Mach number
(Haugen, Brandenburg &
Mee 2004)

Magnetic energy growth rates

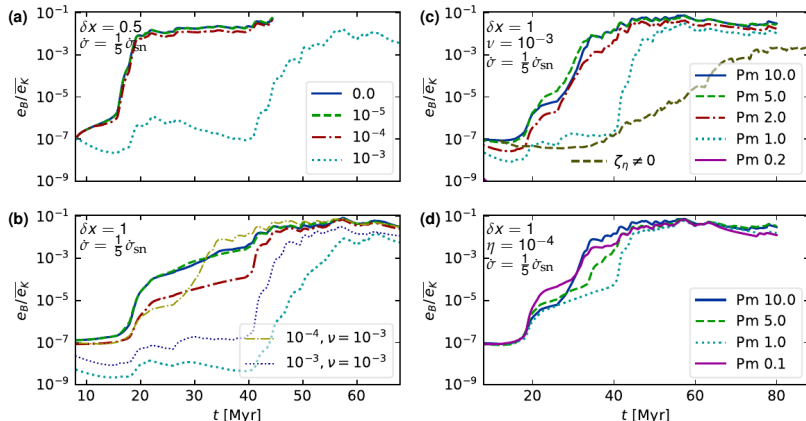
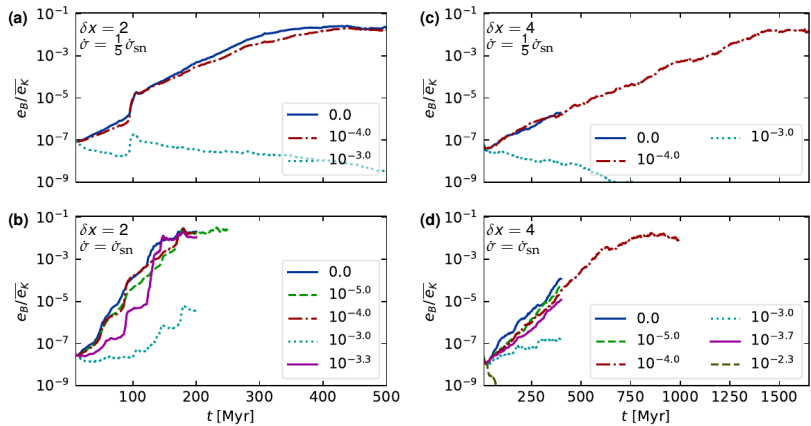


Figure: Magnetic energy density e_B normalized by the time-averaged kinetic energy $\overline{e_K}$ for various resistivities η for values given in each panel of resolution δx and SN rate $\dot{\sigma}$ normalized by the solar neighborhood rate $\dot{\sigma}_{\text{sn}} \simeq 50 \text{ kpc}^{-3} \text{ Myr}^{-1}$. $\nu = 0$, except where Pm is varied with ν fixed (c) or η fixed (d). **Dependence on Pm** (Haugen, Brandenburg & Dobler 2004)

Magnetic energy growth rates



caption magnetic energy density e_B normalized by the time-averaged kinetic energy \bar{e}_K for various resistivities η for values given in each panel of resolution δx and SN rate $\dot{\sigma}$ normalized by the solar neighborhood rate $\dot{\sigma}_{\text{sn}} \simeq 50 \text{ kpc}^{-3} \text{ Myr}^{-1}$. $\nu = 0$ η fixed (d).

Energy spectra by resolution and resistivity

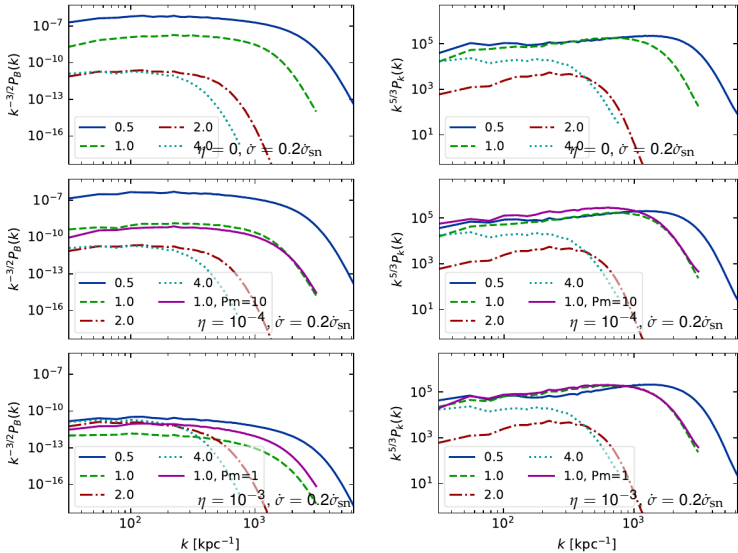


Figure: Compensated power spectra magnetic (left) and kinetic (right). Resistivity η & supernova rate $\dot{\sigma}$, 19.5 Myr ($\delta x = 0.5, 1$ pc), 100 Myr (2, 4 pc).

Multi-phase structure of SSD

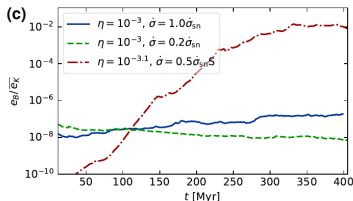
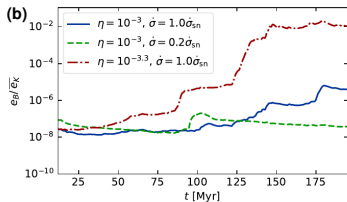
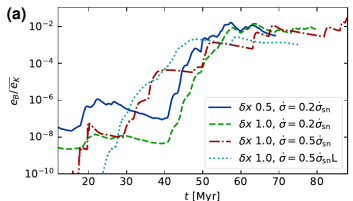
Magnetic energy growth
mainly associated with
warm gas

Occasional rapid
acceleration in mature
hot bubbles (Gent
et al. 2021)

Experimental setup

- ▶ Sliding periodic ISM horizontally $L_x = 512$ pc $L_z = 3072$ pc and $L_y = 512, 1024$ and 1536 pc (Mean field suppressed with 512)
- ▶ 1 ppcc initially at the midplane
- ▶ SN rate compared to solar neighbourhood $0.3 - 0.8 \dot{\sigma}_{\text{sn}}$ to reduce mass loss (eventually use mass conservation)
- ▶ Energy: UV-heating varied to support disk with pressure missing from CR, ionization
- ▶ Resolution 1, and 4 pc

Magnetic energy SSD growth - domain effects



(a) High resolution simulations confirm SSD unconstrained by domain $L_y \simeq 128$ pc (periodic boxes).

(b) Low resolution dynamo growth dependence on resistivity and SN rate $\dot{\sigma}$ (periodic boxes).

(c) Low resolution SSD more efficient in stratified ISM vs periodic box.

Thin disk ISM with large scale rotation and shear

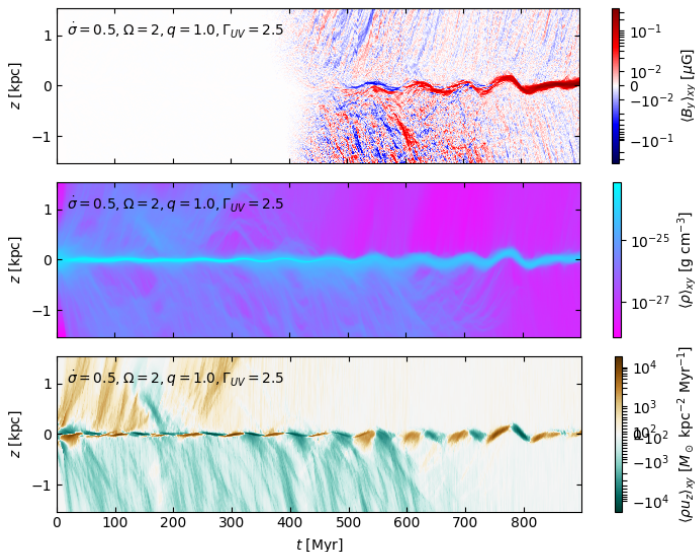


Figure: Horizontal averages 4 pc resolution with UV-heating Γ_{UV} 2.5 times the solar vicinity model

Interdependence of SSD and LSD

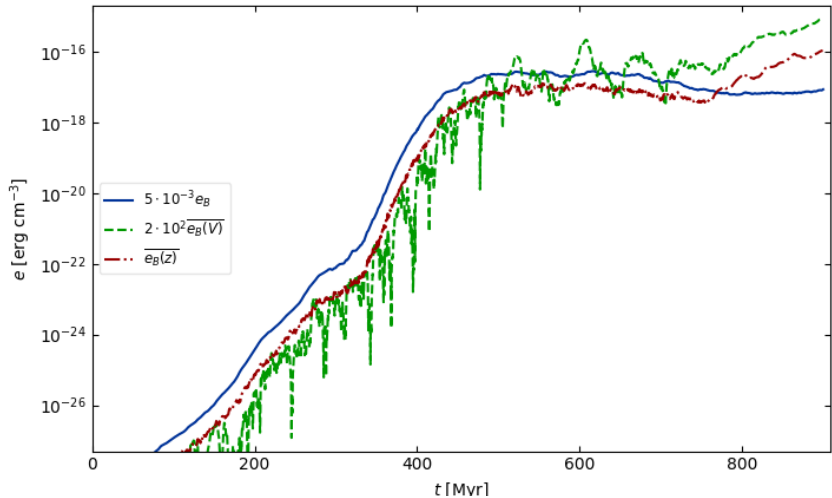


Figure: Energy of the total and mean magnetic field $\Gamma_{UV} = 2.5$

Thick disk ISM with large scale rotation and shear

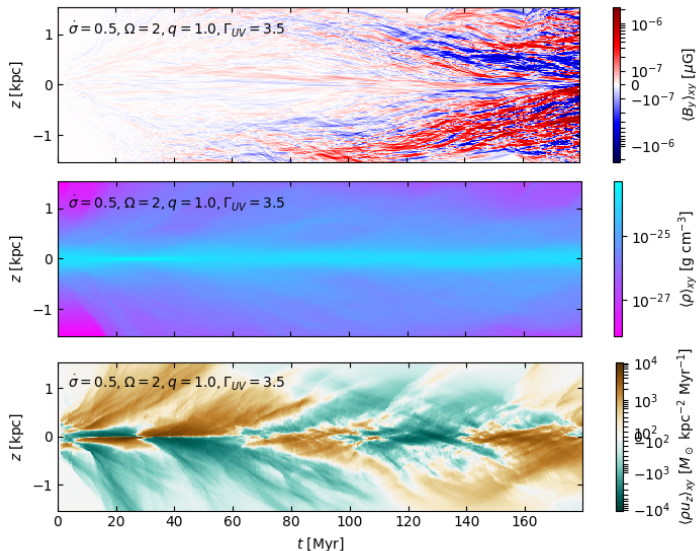


Figure: Horizontal averages 4 pc resolution with UV-heating Γ_{UV} 3.5 times the solar vicinity model

Large scale dynamo

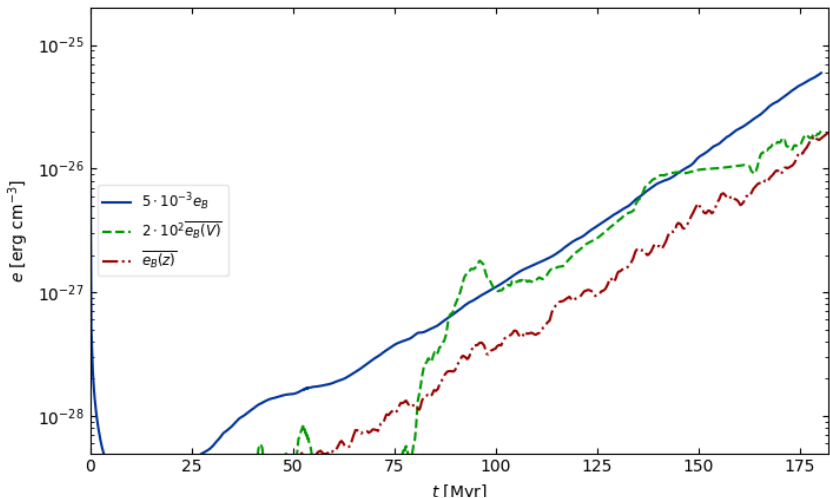


Figure: Energy of the total and mean magnetic field $\Gamma_{UV} = 3.5$.
Growth 2 orders of magnitude in 100 Myr

Summary of results

- ▶ SN turbulence convergent for $\delta x \lesssim 1$ pc
- ▶ SSD is very easily excited in the ISM - [contrast isothermal high \(Haugen, Brandenburg & Mee 2004\)](#)
- ▶ (Balsara et al. 2004) experiment confirmed as SSD and not tangling
- ▶ Critical dynamo number and growth rates not clearly P_m or R_m dependent in multi-phase ISM [contrast isothermal SSD \(Haugen, Brandenburg & Dobler 2004\)](#) – (Käpylä et al. 2018) baroclinic effects vs (Federrath et al. 2011)
- ▶ For $\dot{\sigma} \in (0.2\dot{\sigma}_{sn}, 8\dot{\sigma}_{sn})$ SSD critical dynamo number decreases with $\dot{\sigma}_{sn}$
- ▶ SSD saturates at $\sim 5\%$ energy equipartition independent of R_m or δx , depends on resistivity η for constant ν
- ▶ LSD during SSD kinematic phase dependent of SSD. In non-linear stage LSD exponential.
- ▶ Effect of resolution Reynolds numbers effect SSD (indirectly early LSD). Hi resolution confirmation of LSD growth rate unconfirmed.

Bibliography I

- Balsara D S, Kim J, Mac Low M M & Mathews G J 2004 *ApJ* **617**(1), 339–349.
- Federrath C, Chabrier G, Schober J, Banerjee R, Klessen R S & Schleicher D R G 2011 *Physical Review Letters* **107**(11), 114504.
- Gent F A, Mac Low M M, Käpylä M J & Singh N K 2021 *ApJ Letters* **910**(2), L15.
- Gent F A, Shukurov A, Sarson G R, Fletcher A & Mantere M J 2013 *MNRAS* **430**, L40–L44.
- Gressel O & Elstner D 2020 *MNRAS* **494**(1), 1180–1188.
- Gressel O, Ziegler U, Elstner D & Rüdiger G 2008 *Astronomische Nachrichten* **329**, 619.
- Hanasz M, Wóltanowski D & Kowalik K 2009 *ApJ Letters* **706**(1), L155–L159.
- Haugen N E, Brandenburg A & Dobler W 2004 *Physical Review E* **70**(1), 016308.
- Haugen N E L, Brandenburg A & Mee A J 2004 *MNRAS* **353**, 947–952.
- Käpylä M J, Gent F A, Väisälä M S & Sarson G R 2018 *A&A* **611**, A15.
- Korpi M J, Brandenburg A, Shukurov A & Tuominen I 1999 *A&A* **350**, 230–239.

Bibliography II

- Pakmor R, Gómez F A, Grand R J J, Marinacci F, Simpson C M, Springel V, Campbell D J R, Frenk C S, Guillet T, Pfrommer C & White S D M 2017 *MNRAS* **469**(3), 3185–3199.
- Rieder M & Teyssier R 2016 *MNRAS* **457**(2), 1722–1738.
- Rieder M & Teyssier R 2017a *MNRAS* **471**(3), 2674–2686.
- Rieder M & Teyssier R 2017b *MNRAS* **472**(4), 4368–4373.
- Steinwandel U P, Beck M C, Arth A, Dolag K, Moster B P & Nielaba P 2019 *MNRAS* **483**(1), 1008–1028.
- Wang P & Abel T 2009 *ApJ* **696**(1), 96–109.

acknowledgements

The authors wish to acknowledge CSC – IT Center for Science, Finland, for computational resources Grand Challenge GDYNS Project 2001062. M-MML was partly supported by US NSF grant AST18-15461. FAG and MJK acknowledge support of the Academy of Finland ReSoLVE Centre of Excellence (grant number 307411). This project has received funding from the European Research Council (ERC) under the European Union’s Horizon 2020 research and innovation programme (Project UniSDyn, grant agreement no: 818665).

Software: Pencil Code

- ▶ Brandenburg A & Dobler W 2002 Computer Physics Communications 147(1-2), 471–475.
- ▶ Brandenburg A, Johansen A, Bourdin P A, Dobler W, Lyra W, Rheinhardt M, Bingert S, Haugen N E L, Mee A, Gent F, Babkovskaia N, Yang C C, Heinemann T, Dintrans B, Mitra D, Candelaresi S, Warnecke J, Käpylä, P J, Schreiber A, Chatterjee P, Käpylä M J, Li X Y, Krüger J, Aarnes J R, Sarson G R, Oishi J S, Schober J, Plisson R, Sandin C, Karchniwy E, Rodrigues L F S, Hubbard A, Guerrero G, Snodin A, Losada I R, Pekkilä J & Qian C 2020 arXiv e-prints p. arXiv:2009.08231.

Growth in warm/hot gas

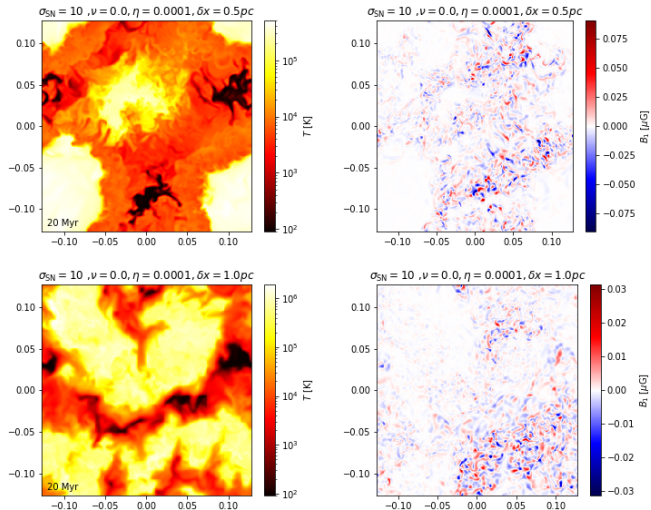


Figure: Slices for resolution of 0.5 pc and 1 pc sampled from the kinematic dynamo state.